



## A case study into the measurement of ship emissions from plume intercepts of the NOAA ship *Miller Freeman*

C. D. Cappa<sup>1</sup>, E. J. Williams<sup>2,3</sup>, D. A. Lack<sup>2,3</sup>, G. M. Buffaloe<sup>1</sup>, D. Coffman<sup>7</sup>, K. L. Hayden<sup>5</sup>, S. C. Herndon<sup>4</sup>, B. M. Lerner<sup>2,3</sup>, S.-M. Li<sup>5</sup>, P. Massoli<sup>4</sup>, R. McLaren<sup>6</sup>, I. Nuaaman<sup>5,6</sup>, T. B. Onasch<sup>4</sup>, and P. K. Quinn<sup>7</sup>

<sup>1</sup>Department of Civil and Environmental Engineering, University of California, Davis, California, 95616, USA

<sup>2</sup>NOAA Earth System Research Laboratory, Boulder, Colorado, 80305, USA

<sup>3</sup>Cooperative Institute for Research in Environmental Sciences, University of Colorado, Boulder, Colorado, 80305, USA

<sup>4</sup>Aerodyne Research, Inc., Billerica, Massachusetts, 01821, USA

<sup>5</sup>Air Quality Research Division, Environment Canada, 4905 Dufferin St., Toronto, M3H5T4, Canada

<sup>6</sup>Centre for Atmospheric Chemistry, York University, 4700 Keele St., Toronto, M3J1P3, Canada

<sup>7</sup>NOAA Pacific Marine Environment Laboratory, Seattle, Washington, 98115, USA

Correspondence to: C. D. Cappa (cdcappa@ucdavis.edu)

Received: 15 August 2013 – Published in Atmos. Chem. Phys. Discuss.: 23 September 2013

Revised: 16 December 2013 – Accepted: 2 January 2014 – Published: 5 February 2014

**Abstract.** Emissions factors (EFs) for gas and sub-micron particle-phase species were measured in intercepted plumes as a function of vessel speed from an underway research vessel, the NOAA ship *Miller Freeman*, operating a medium-speed diesel engine on low-sulfur marine gas oil (fuel sulfur content  $\sim 0.1\%$  by weight). The low-sulfur fuel in use conforms to the MARPOL fuel sulfur limit within emission control areas set to take effect in 2015 and to California-specific limits set to take effect in 2014. For many of the particle-phase species, EFs were determined using multiple measurement methodologies, allowing for an assessment of how well EFs from different techniques agree. The total sub-micron PM ( $PM_{10}$ ) was dominated by particulate black carbon (BC) and particulate organic matter (POM), with an average POM/BC ratio of 1.3. Consideration of the POM/BC ratios observed here with literature studies suggests that laboratory and in-stack measurement methods may overestimate primary POM EFs relative to those observed in emitted plumes. Comparison of four different methods for black carbon measurement indicates that careful attention must be paid to instrument limitations and biases when assessing  $EF_{BC}$ . Particulate sulfate ( $SO_4^{2-}$ ) EFs were extremely small and the particles emitted by *Miller Freeman* were inefficient as cloud condensation nuclei (CCN), even at high super saturations, consistent with the use of very low-sulfur fuel and the overall small emitted particle sizes. All measure-

ment methodologies consistently demonstrate that the measured EFs (fuel mass basis) for  $PM_{10}$  mass, BC and POM decreased as the ship slowed. Particle number EFs were approximately constant across the speed change, with a shift towards smaller particles being emitted at slower speeds. Emissions factors for gas-phase CO and formaldehyde (HCHO) both increased as the vessel slowed, while EFs for  $NO_x$  decreased and  $SO_2$  EFs were approximately constant.

### 1 Introduction

Emissions of particulate matter (PM) and trace gases from ships operating in the open ocean as well as in coastal and inland waterway areas have significant impacts on air quality and climate (Corbett et al., 2007; Fuglestvedt et al., 2009). Quantification of these impacts requires use of detailed emissions inventories and the specification of emission factors (EFs) to determine the spatial distribution of emissions. Emission factors for ships are commonly determined from (i) direct stack sampling of in-use ships, (ii) interception of emitted plumes from in-use ships or (iii) from test engines in laboratories. Various studies indicate that EFs for total PM and different PM species can be highly variable between different ships. This variability reflects real differences in ship operation and the resulting emissions, but may also reflect

differences between the measurement or sampling methodologies employed between different studies. Detailed characterization of the emissions from a single ship using multiple measurement techniques for a given species can facilitate understanding of the role that methodological differences play in determining measured EFs.

In addition, changes in engine load, which often correspond to changes in vessel speed, are known (Lloyd's Register Engineering Services, 1995) to have a large influence on the overall efficiency of the combustion process, with fuel economy ( $F_{\text{econ}}$ ; e.g., km (kg fuel)<sup>-1</sup>) often increasing with decreasing speed and engine load. This increase in fuel efficiency generally translates to a decrease in emissions for a given pollutant, however the magnitude of the change is modified by the specific response of the emission factor for that pollutant to the change in speed (Lack et al., 2011). Such efficiency gains have motivated consideration and implementation of speed restrictions (or a fuel tax aimed at speed reduction) near some coastal and port regions or along shipping routes (Corbett et al., 2009; Buhaug et al., 2009). Most such efforts are aimed at decreasing emissions from large ocean-going vessels. However, the operation of smaller crafts near coastal regions and inland waterways also contributes to local pollution (Corbett and Fischbeck, 2000), and thus the dependence of their emissions on vessel speed must also be understood so that appropriate pollution control strategies in those regions can be developed. This is particularly the case for smaller vessels that are likely to operate at speeds and engine loads that are more variable than large ocean-going vessels. Furthermore, vessels that operate in shorter time-frame service operations near coastal environments have highly variable load distributions and ages, and thus it is necessary to characterize emissions factors and their speed dependence for both newer and older vessels. Development of next-generation emissions inventories will result from such higher-resolution assessments of the dependence of and variations in engine load distributions, fleet age and emission factor with engine load, engine age and vessel speed (Wang and Minjares, 2013).

Here, we report measurements of both PM and gas-phase EF values for a series of plumes emitted by the NOAA ship *Miller Freeman*, which was in transit within regulated waters off the coast of Santa Barbara, CA and intercepted during the 2010 CalNex field campaign (Ryerson et al., 2013). Regulated waters correspond to the region within 24 nautical miles of the CA baseline where, as of 1 July 2009, ocean-going vessels were required to utilize fuels with  $\leq 1.5\%$  sulfur (California Air Resources Board, 2011). (The fuel sulfur requirement has since been reduced to  $\leq 1\%$ , as of August 2012 and will further decrease to  $\leq 0.1\%$  in 2014.) The PM measurements were made using a suite of different measurement techniques, some of which overlap in terms of the specific PM species measured. In addition, the intercepted plumes were emitted while the *Miller Freeman* operated at four different but constant speeds, and thus enables an as-

essment of the influence of vessel speed on the emissions from vessels of this type. The *Miller Freeman* is a 65.5 m (215 ft) fisheries and oceanographic research vessel with a cruising speed of 11 knots operating a controllable pitch propeller (NOAA, 2010). The single main engine is a 1.64 MW, 2-stroke, geared medium-speed diesel (MSD) with variable-speed operation from General Electric that is equipped with a blower and has a rated power of 2.2 khp (= 1.47 kW). The *Miller Freeman* is an older vessel, launched in 1967, that was decommissioned in 2013. During the plume intercepts the *Miller Freeman* was operating on a mix of "ultra-low sulfur diesel from California mixed with standard marine diesel from Washington [state]" (P. Murphy, personal communication, 2010). Fuel samples were not available for off-line analyses, but as we show later the fuel sulfur content is estimated to be around 0.1% by weight, consistent with marine gas oil (MGO) or marine distillate oil (MDO) fuels, which will be referred to generically as low-sulfur fuels (LSF). The low-sulfur fuel in use conforms to the International Convention for the Prevention of Pollution from Ships (MARPOL) fuel sulfur limit within emission control areas set to take effect in 2015 (International Maritime Organization, 2013) and to California-specific limits set to take effect in 2014 (California Air Resources Board, 2011).

The measurements reported here therefore provide a case study allowing for assessment of how well different measurement techniques agree in terms of the derived EFs and for the influence of vessel speed on older, smaller MSD vessels operating on LSF, which are an important class of vessels that operate in near-coastal and inland waterways. For example, plumes were encountered for a number of other MSD vessels with build years ranging from 1952 to 2006 during CalNex, with most of these being pre-1990 vessels. This is generally consistent with the average age (as of 2010) of "other" vessels (i.e., exclusive of container, bulk, cargo and tanker vessels) in the world merchant fleet being 25 yr (United Nations Conference on Trade and Development, 2011) and with 43% of such vessels (i.e., passenger, offshore, service and tugs) in 2011 being older than 25 yr (Equasis, 2012). Further, larger ocean-going vessels are increasingly having to switch to LSFs from the commonly used high-sulfur heavy fuel oil (HFO, or bunker fuel) during operation near coasts (US EPA, 2010; California Air Resources Board, 2011). (Although there were plumes from many other ships intercepted during CalNex, not all instruments were operating at all times under conditions that allow for determination of EFs, and thus we restrict this study to the ship for which the most comprehensive measurements are available.) The results here are compared with literature results from test-rig, in-stack and plume studies to place them in the broader context that is necessary for development of next-generation emissions inventories.

## 2 Experimental

Emissions factors for PM and trace gases (CO, SO<sub>2</sub>, HCHO and NO<sub>x</sub>) were measured using the plume intercept method (also known as the “sniffer” method), wherein concentrations of the pollutants are measured in a plume that is intercepted downwind of the vessel of interest, here the *Miller Freeman*. One benefit of the plume intercept method is that atmospherically relevant dilution factors and temperatures are achieved by the time the plume is sampled, although the exact extent of dilution varies for each plume and the plume must be identifiable above background concentrations. Gas-phase and PM measurements were made onboard the NOAA-sponsored Woods Hole R/V *Atlantis* as part of the CalNex field campaign (Ryerson et al., 2013). The emissions plume from *Miller Freeman* was intercepted on five occasions on 19 May 2010, with *Miller Freeman* traveling at four different speeds: 2.9 knots, 6.9 knots (twice), 10.2 knots and 12 knots. The coordinated effort between the ships allowed for measurements to be made in plumes that were emitted when *Miller Freeman* was traveling at a constant speed. Plumes from *Miller Freeman* were identified by combining the relative ship positions with the local wind direction and wind speed data measured from *Atlantis*. Using these data, local back-trajectories from *Atlantis* were computed by simple vector analysis to determine the location of and speed at which *Miller Freeman* was cruising at the time the pollutants were emitted and to estimate the age of each plume encountered. Separation distances between the ships were from 200 to 900 m; plume travel times were from 1 to 5 min (Table 1). Engine load ( $F_{\text{load}}$ ) information is not directly available from the *Miller Freeman*. For marine vessels engine load is often estimated from the vessel speed ( $u$ ) using a cubic power law relationship (the so-called propeller law), where  $F_{\text{load}} = (u_{\text{actual}} / u_{\text{max}})^3$  (Corbett et al., 2009). However, because the *Miller Freeman* operated a controllable pitch propeller, as opposed to a fixed pitch propeller, the power law is likely not appropriate. Nonetheless, estimated engine load values from the propeller law are reported here for reference. We assume that the maximum speed encountered here, 12 knots, corresponds to  $u_{\text{max}}$ ; the  $F_{\text{load}}$  values are then 1.4 %, 19 %, 61 % and 100 %, respectively. This lowest  $F_{\text{load}}$  value is lower than typical values under idling conditions, indicating a likely failure of the propeller law for this vessel. The encounter occurred during late afternoon when the temperature was between 11.9 °C and 12.2 °C and the relative humidity was between 88 % and 93 % (although particles were dried before sampling).

A table listing the instrumentation used as part of this study is provided in the Supplement. Gas-phase measurements included CO<sub>2</sub>, NO<sub>x</sub>, CO, SO<sub>2</sub> and HCHO with uncertainties of ±0.25 ppmv, ±20 %, ±4.1 % and ±15 % and ±9 %, respectively (Williams et al., 2009). Particle-phase instrumentation included a high-resolution time-of-flight aerosol mass spectrometer (HR-AMS) for measurement of

particulate SO<sub>4</sub><sup>2-</sup>, NO<sub>3</sub><sup>-</sup>, NH<sub>4</sub><sup>+</sup>, Cl<sup>-</sup> and particulate organic matter (POM), a single particle soot photometer (SP2) for refractory BC (rBC) particle mass and number concentrations and size distributions (Schwarz et al., 2006), a soot-particle AMS (SP-AMS) for refractory BC particle mass and POM and SO<sub>4</sub><sup>2-</sup>, NO<sub>3</sub><sup>-</sup>, NH<sub>4</sub><sup>+</sup> and Cl<sup>-</sup> coating mass concentrations (Onasch et al., 2012), an ultrafine (CN > 3 nm; TSI model 3025) and mixing (CN > 12 nm; Brechtel Manufacturing) condensation particle counter (CPC) for particle condensation nuclei (CN) number concentrations, a cloud condensation nuclei (CCN) counter (Roberts and Nenes, 2005), a photo-acoustic spectrometer (PAS, operating at 532 nm and 405 nm) for light absorption (Lack et al., 2012), one three-wavelength particle soot absorption photometer (PSAP, at 450, 530 and 700 nm) for light absorption (Virkkula et al., 2005), a cavity ringdown spectrometer (CRD, at 532 nm) for light extinction and optical hygroscopicity measurements (Langridge et al., 2011) and a scanning mobility particle sizer (SMPS) for particle size distribution measurement operating with a scan time of 2.5 min. Corrections to the HR-AMS and SP-AMS to account for the instrumental CE are required. For the HR-AMS, a CE < 1 is mostly caused by bounce of particles from the internal vaporizer surface (Huffman et al., 2005; Matthew et al., 2008). For the HR-AMS, a collection efficiency (CE) of 1.0 has been assumed; this means that the EFs determined from this instrument are lower limits. While the CE for HR-AMS is mostly caused by particle bounce, the CE in the SP-AMS is primarily a function of the degree of overlap between the particle and laser beams and the laser power profile in the overlapping region (Onasch et al., 2012). For the SP-AMS, a CE for rBC of 0.2 ± 40 % is used while a CE = 0.4 ± 100 % is used for non-rBC components that are internally mixed with rBC (see Supplement). Note that the precision of the measured rBC and non-rBC species concentrations is substantially better than the above uncertainties indicate, which account for measurement accuracy. The SP2 was calibrated using fullerene soot particles, which have been shown to give a similar response as diesel soot (Laborde et al., 2012). The SP2 measured particles with volume equivalent diameters ( $d_{p, \text{VED}}$ ) between 60 nm and 300 nm. The SP2 rBC concentrations were corrected for the measured particle detection efficiency of 0.7 for particles with  $d_{p, \text{VED}} > 100$  nm. For  $d_{p, \text{VED}} \leq 100$  nm, a size-dependent detection efficiency was applied to the data to account for the fall off in instrument sensitivity (see Supplement; Schwarz et al., 2010; Liggió et al., 2012). Overall uncertainties for the particle measurement instrumentation are estimated to be +35 % / - 15 % (HR-AMS), +100 % / - 20 % (SP2), ±40 % (SP-AMS, rBC), ±100 % (SP-AMS; non-BC), ±5 % (CN), ±10 % (CCN), ±7 % (PAS, 532 nm), ±15 % (PAS, 405 nm), ±20 % (PSAP) and ±1 % (CRD), when signals are well above their detection limits. Plume-specific detection limits, given as  $DL = 3\sigma / \sqrt{N}$ , were assessed, where  $\sigma$  is the standard deviation observed during the background

**Table 1.** Measured emissions factors for the NOAA ship *Miller Freeman* as a function of vessel speed.

Speed	2.9 knots	6.9 knots	6.9 knots	10.2 knots	12 knots	Units
Approx. plume age	5	2	1	1	3	Minutes
Gas phase						
NO <sub>x</sub> <sup>a</sup>	45.6 ± 8.2	45.7 ± 8.2		53.3 ± 9.6	61.1 ± 11.0	g (kg fuel) <sup>-1</sup>
SO <sub>2</sub>	1.85 ± 0.5	1.76 ± 0.44		1.88 ± 0.47	2.27 ± 0.57	g (kg fuel) <sup>-1</sup>
CO	6.23 ± 1.2	5.83 ± 0.9		2.92 ± 0.58	2.50 ± 0.50	g (kg fuel) <sup>-1</sup>
HCHO	0.25 ± 0.04	0.125 ± 0.02		0.058 ± 0.01	0.056 ± 0.02	g (kg fuel) <sup>-1</sup>
Particle phase						
SO <sub>4</sub> <sup>2-</sup> (HR-AMS)	< 0.05 <sup>j</sup>	< 0.15	< 0.09	< 0.10	< 0.13	g (kg fuel) <sup>-1</sup>
SO <sub>4</sub> <sup>2-</sup> (SP-AMS)	< 0.03	< 0.06	< 0.05	< 0.05	< 0.07	g (kg fuel) <sup>-1</sup>
OM (HR-AMS)	0.07	0.10	0.18	0.47	1.13	g (kg fuel) <sup>-1</sup>
OM (SP-AMS)	< 0.03	0.19	0.23	0.53	0.86	g (kg fuel) <sup>-1</sup>
OM (Wt. Ave)	0.05	0.10	0.18	0.47	1.10	g (kg fuel) <sup>-1</sup>
NO <sub>3</sub> <sup>-</sup> (HR-AMS)	< 0.004	< 0.012	< 0.008	< 0.006	< 0.011	g (kg fuel) <sup>-1</sup>
NO <sub>3</sub> <sup>-</sup> (SP-AMS)	< 0.002	< 0.004	< 0.004	< 0.003	< 0.005	g (kg fuel) <sup>-1</sup>
NH <sub>4</sub> <sup>+</sup> (HR-AMS)	< 0.02	< 0.07	< 0.03	< 0.04	< 0.05	g (kg fuel) <sup>-1</sup>
NH <sub>4</sub> <sup>+</sup> (SP-AMS)	< 0.004	< 0.006	0.003	0.003	< 0.009	g (kg fuel) <sup>-1</sup>
Cl <sup>-</sup> (HR-AMS)	< 0.002	< 0.005	< 0.003	< 0.004	0.002	g (kg fuel) <sup>-1</sup>
Cl <sup>-</sup> (SP-AMS)	< 0.002	< 0.004	< 0.003	< 0.003	0.003	g (kg fuel) <sup>-1</sup>
rBC (SP2)	0.008	0.09	0.11	0.30	0.16	g (kg fuel) <sup>-1</sup>
rBC (SP-AMS)	0.06	0.15	0.14	0.34	0.43	g (kg fuel) <sup>-1</sup>
eBC (PAS,G) <sup>b</sup>	0.04	0.14	0.20	0.39	0.41	g (kg fuel) <sup>-1</sup>
eBC (PAS,B) <sup>c</sup>	0.16	0.19	0.27	0.47	0.52	g (kg fuel) <sup>-1</sup>
eBC (PSAP, Ave) <sup>d</sup>	0.04	0.19	0.23	0.49	0.48	g (kg fuel) <sup>-1</sup>
BC (Wt. Ave) <sup>k</sup>	0.04	0.15	0.20	0.41	0.41	g (kg fuel) <sup>-1</sup>
CN (> 12 nm)	1.33 × 10 <sup>16</sup>	1.04 × 10 <sup>16</sup>	1.61 × 10 <sup>16</sup>	1.95 × 10 <sup>16</sup>	1.48 × 10 <sup>16</sup>	# (kg fuel) <sup>-1</sup>
CN (> 3 nm)	1.93 × 10 <sup>16</sup>	1.72 × 10 <sup>16</sup>	2.65 × 10 <sup>16</sup>	3.06 × 10 <sup>16</sup>	2.23 × 10 <sup>16</sup>	# (kg fuel) <sup>-1</sup>
CCN <sup>e</sup> (SS = 0.7 %)	2.6 × 10 <sup>14</sup>	–	3.6 × 10 <sup>14</sup>	–	1.7 × 10 <sup>14</sup>	# (kg fuel) <sup>-1</sup>
CCN (SS = 0.6 %)	8.3 × 10 <sup>13</sup>	–	7.0 × 10 <sup>13</sup>	–	6.3 × 10 <sup>13</sup>	# (kg fuel) <sup>-1</sup>
CCN (SS = 0.4 %)	–	2.7 × 10 <sup>13</sup>	–	–	–	# (kg fuel) <sup>-1</sup>
CCN (SS = 0.3 %)	–	–	–	< 1 × 10 <sup>13</sup>	–	# (kg fuel) <sup>-1</sup>
CCN/CN <sup>f</sup> (SS = 0.7 %)	0.021	–	0.019	–	0.008	unitless
CCN/CN (SS = 0.6 %)	0.007	–	0.004	–	0.004	unitless
CCN/CN (SS = 0.4 %)	–	0.002	–	–	–	unitless
CCN/CN (SS = 0.3 %)	–	–	–	< 4 × 10 <sup>-4</sup>	–	unitless
Extinction	0.83	1.60	2.10	3.37	4.05	m <sup>2</sup> (kg fuel) <sup>-1</sup>
PM <sub>1</sub> (ext.) <sup>h</sup>	0.21	0.40	0.52	0.84	1.01	g (kg fuel) <sup>-1</sup>
PM <sub>1</sub> (sum) <sup>g</sup>	0.09	0.25	0.38	0.88	1.51	g (kg fuel) <sup>-1</sup>
D <sub>p,m</sub> <sup>i</sup>	30	–	–	48	69	nm

<sup>a</sup>Calculated as equivalent NO<sub>2</sub>; <sup>b</sup>Assumes MAE = 7.75 m<sup>2</sup> g<sup>-1</sup>; <sup>c</sup>Assumes MAE = 10.2 m<sup>2</sup> g<sup>-1</sup>; <sup>d</sup>Assumes MAE = 7.5 m<sup>2</sup> g<sup>-1</sup>; <sup>e</sup>CCN measurements may only be for a portion of a given plume due to the time-dependent supersaturation; <sup>f</sup>CCN/CN ratios have been calculated after determining CN EFs over the same period as the CCN, and therefore may not correspond to the reported plume-average CN EFs; <sup>g</sup>[PM<sub>1</sub>] = [OM]<sub>ave</sub> + [BC]<sub>ave</sub>; <sup>h</sup>Assumes MEE = 4 m<sup>2</sup> g<sup>-1</sup>; <sup>i</sup>Number-weighted mobility diameter; <sup>j</sup>Values reported as < X are the plume-specific detection limit; <sup>k</sup>Uncertainty weighted average.

periods just before/after the plume and  $N$  is the number of data points across an individual plume. Typical values of  $N$  were around 70 points per plume, except for CCN (see Supplement). Absolute EF values are only reported when the in-plume signals were above the detection limit.

Particle-phase EFs were determined using an area-ratio approach, where the background-subtracted area under the

ship plume (i.e., plotted as concentration vs. time) for the pollutant of interest is divided by the similarly calculated area under the CO<sub>2</sub> plume. The ratio gives the EF after appropriate unit conversion and multiplication by the mass fraction of carbon in the fuel, which was assumed to be 0.865 (Lack

et al., 2009; Williams et al., 2009). Specifically,

$$EF_X = \frac{A_{X,\text{bgd}}}{A_{\text{CO}_2,\text{bgd}}} \cdot f_{\text{fuel}}, \quad (1)$$

where  $A_{X,\text{bgd}}$  is the background-subtracted concentration of species X, integrated over the entire plume,  $A_{\text{CO}_2,\text{bgd}}$  is the same for  $\text{CO}_2$  and  $f_{\text{fuel}}$  is the conversion factor between  $\text{CO}_2$  (in ppmv) and fuel consumed (kg fuel). The area-ratio approach is independent of the time-resolution of the instrumentation (which differs between different instruments) and has been used in other studies for calculating emission ratios of ship emissions (McLaren et al., 2012). Importantly, in the plume intercept method dilution is naturally accounted for because the pollutant of interest is ratioed to  $\text{CO}_2$  concentrations, and  $\text{CO}_2$  is non-reactive within the plume. Gas-phase EFs were determined using linear regression analysis since the time-resolution of all gas-phase instruments was identical and the area-ratio and linear regression methods give nearly identical results (Williams et al., 2009). Although fuel carbon is also emitted as CO, combustion-related hydrocarbons and particulate carbon, the majority of carbon is emitted as  $\text{CO}_2$  (> 99 %, based on the derived EFs), and thus the determination of the various EFs using only  $\text{CO}_2$  will lead to negligible biases. Given our method of determination, the EFs reported are related to the mass of fuel consumed, with units of emissions of X per kg of fuel (where emissions of X can be in grams, particles, etc.).

Conversion of the optical property measurements to mass equivalent EFs requires specification of the mass absorption or mass extinction efficiency (MAE or MEE). Specifically, division of the measured extinction coefficient by the MEE yields the mass concentration of  $\text{PM}_{10}$ , while division of the measured absorption coefficient by the MAE yields the mass concentration of equivalent BC (eBC; Petzold et al., 2013). Here, we use MAE =  $10.2 \text{ m}^2 \text{ g}^{-1}$  (405 nm),  $9.2 \text{ m}^2 \text{ g}^{-1}$  (450 nm),  $7.75 \text{ m}^2 \text{ g}^{-1}$  (532 nm),  $7.5 \text{ m}^2 \text{ g}^{-1}$  (550 nm) and  $5.9 \text{ m}^2 \text{ g}^{-1}$  (700 nm), and MEE =  $4 \text{ m}^2 \text{ g}^{-1}$  (532 nm). The MAE values were specified based on that reported by Bond and Bergstrom (2006) at 550 nm and extrapolated to other wavelengths assuming a  $1/\lambda$  dependence. The MEE values are from Hand and Malm (2007). The uncertainty in the conversion for MAE is  $\sim \pm 15 \%$ , while for MEE it is estimated as at least  $\pm 30 \%$  based on the difference in the MEE between different particle components. Final uncertainties in the EFs were determined for each encounter for each instrument as the larger of the instrument uncertainty or the propagated standard deviation measured during the background (non-plume) period around each plume.

### 3 Results and discussion

#### 3.1 Particle-phase emissions

##### 3.1.1 Mass emission factors

Emissions factors determined for all PM species that were measured are reported in Table 1 and shown in Fig. 1. The results are provided for each of the five plumes that were intercepted, which correspond to different vessel speeds at time of emission. The EF for  $\text{PM}_{10}$  mass was determined either as the uncertainty-weighted sum of the chemically specific measurements that were above detection limits (i.e.,  $EF_{\text{PM}_{10},\text{Sum}} = EF_{\text{BC}} + EF_{\text{POM}}$ , where  $EF_{\text{SO}_4}$  has been excluded because it is below the detection limit for all intercepts) or from the measurement of total light extinction ( $EF_{\text{PM}_{10},\text{Ext}}$ ). Overall, the two methodologies agree within uncertainties for each intercept, although for the three slowest speed intercepts the  $EF_{\text{PM}_{10},\text{Sum}} < EF_{\text{PM}_{10},\text{Ext}}$  with the opposite true for the two highest speed intercepts. This may reflect speed-dependent variations in the POM/BC ratio (discussed further below), which can influence the MEE used to convert light extinction to  $\text{PM}_{10}$  mass. On average, the two methods agreed to within 18 %. It is also evident that the  $EF_{\text{PM}_{10}}$  increases substantially with vessel speed (Fig. 1).

The  $EF_{\text{PM}_{10}}$  is dominated by contributions from POM and BC, with all other measured species, in particular  $\text{SO}_4^{2-}$ , contributing negligibly (Fig. 1). The EF for POM was determined from two independent instruments, the HR-AMS and the SP-AMS. Both methods determine POM concentrations via mass spectrometry, but they differ in their specific operation and, importantly, the SP-AMS as operated during CalNex was only sensitive to POM that existed in BC-containing particles while the HR-AMS measures POM in all particles. The two methods are highly consistent in their general dependence on vessel speed (Fig. 1), and the measured  $EF_{\text{POM}}$  values agreed on average to within 16 % despite the substantial uncertainty on the SP-AMS  $EF_{\text{POM}}$ . This consistency in behavior between the HR-AMS and SP-AMS with vessel speed suggests that a substantial fraction of the emitted POM mass is associated (i.e., internally mixed) with BC. The average  $EF_{\text{POM}}$  ( $0.39 \pm 0.44 \text{ g kg fuel}^{-1}$ ) across all engine speeds is somewhat less than the multi-ship MSD average ( $0.65 \pm 0.44 \text{ g kg fuel}^{-1}$ ) from Lack et al. (2009), although it is important to note that nearly all of the MSD vessels sampled by Lack et al. (2009) were tug boats, which likely have a different emissions profile than a research vessel such as the *Miller Freeman*. As with the  $EF_{\text{PM}_{10}}$ , the  $EF_{\text{POM}}$  increases with vessel speed.

The  $EF_{\text{BC}}$  was determined using four independent methods, two that measured equivalent BC by light absorption measurement (PAS and PSAP), one that measured the laser-induced incandescence by refractory BC-containing particles (SP2) and one that measured the refractory BC concentration via mass spectrometry (SP-AMS) (Petzold et al.,

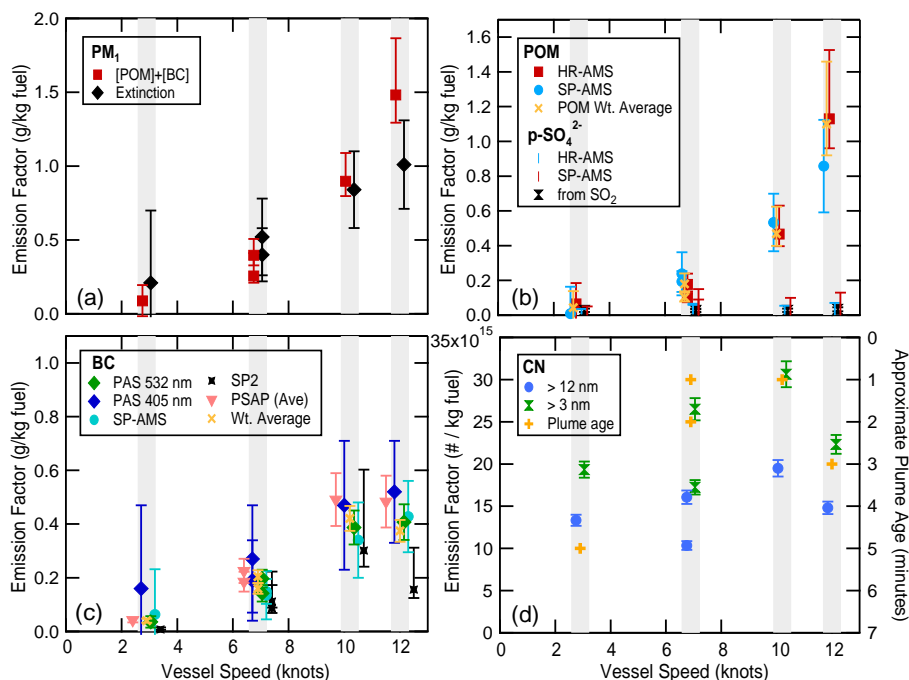


**Fig. 1.** Measured mass or number-based emissions factors (in per kg fuel) for (a) total sub-micron particulate matter, (b) POM or particulate  $\text{SO}_4^{2-}$ , (c) BC, either equivalent BC (PAS and PSAP) or refractory BC (SP2 and SP-AMS) and (d) condensation nuclei and approximate plume age. Values have been offset from the central speed, indicated in gray, for clarity. For sulfate, error bars shown with no data point indicate the plume-specific detection limit for that species.

2013). (We use BC to indicate both eBC and rBC in the discussion that follows, but the distinctions should be kept in mind.) There is good agreement in the  $\text{EF}_{\text{BC}}$  values determined between the two absorption-based methods and the SP-AMS, while the SP2 gave systematically lower values. The good agreement of the PAS- and PSAP-derived  $\text{EF}_{\text{BC}}$  values indicates that positive biases that can be associated with PSAP measurements (Cappa et al., 2008; Lack et al., 2008a) are not significant for the plume particles, most likely because of the relatively large BC content. That the SP2-derived  $\text{EF}_{\text{BC}}$  is systematically lower than that determined using the other methods suggests that a substantial fraction of the BC mass exists in particles with volume equivalent diameters  $d_{p,\text{VED}} < 60$  nm. This is addressed further in Sect. 3.1.3. This suggests that the SP2 may not be suitable for accurate determination of  $\text{EF}_{\text{BC}}$  for fresh ship emissions, although they can provide a lower limit. A similar conclusion has recently been reached by Buffaloe et al. (2013). The weighted-average  $\text{EF}_{\text{BC}}$  ( $0.23 \pm 0.15$  g kg fuel<sup>-1</sup>) across all engine speeds for *Miller Freeman* is on the low end of the multi-ship average ( $0.97 \pm 0.66$  g kg fuel<sup>-1</sup>), determined by Lack et al. (2009) for vessels operating MSD engines. Again, this difference may reflect the difference between the *Miller Freeman* and the predominately tug boats sampled by Lack et al. (2009). As with the  $\text{EF}_{\text{POM}}$ , the  $\text{EF}_{\text{BC}}$  are observed to increase with vessel speed, although somewhat less steeply.

The  $\text{EF}_{\text{SO}_4}$  measurements from the HR-AMS and SP-AMS were below the detection limit at all speeds, and indicate that the  $\text{SO}_4^{2-}$  contribution to the total particle mass is small, consistent with the use of low-sulfur fuel.  $\text{EF}_{\text{SO}_4}$  can also be estimated from the measured  $\text{EF}_{\text{SO}_2}$  (Sect. 3.2) based on previous results that indicate the percent conversion of  $\text{SO}_2$  to  $\text{p-SO}_4^{2-}$  in ship plumes from MSD vessels on the timescales considered here (a few minutes) is  $\sim 1$ – $2$  % (Lack et al., 2009). This yields  $\text{EF}_{\text{SO}_4} = 0.02$ – $0.04$  g kg fuel<sup>-1</sup>, consistent with the directly measured  $\text{EF}_{\text{SO}_4}$  being below the plume-specific detection limits of the HR-AMS and SP-AMS (Table 1). As with  $\text{p-SO}_4^{2-}$ , EFs for particulate  $\text{NO}_3^-$ ,  $\text{NH}_4^+$  and  $\text{Cl}^-$  were at or below the detection limits.

### 3.1.2 The POM/BC ratio

The average particle composition calculated from the weighted average  $\text{EF}_{\text{POM}}$  and  $\text{EF}_{\text{BC}}$ , assuming only BC and POM contribute significantly to PM, is  $53(\pm 14)\%$  POM and  $47(\pm 14)\%$  BC, or  $\text{POM}/\text{BC} = 1.34(\pm 0.9)$  (Fig. 2). The uncertainty on the 2.9 knot plume is large. If this plume is excluded, the fraction of the  $\text{PM}_1$  mass that is POM is observed to increase slightly as vessel speed increases, with  $\text{POM}/\text{BC}$  ranging from 0.6 (6.9 knots) to 3.0 (12 knots), with an average of 1.41. This is a result of the  $\text{EF}_{\text{BC}}$  increasing less steeply with ship speed than  $\text{EF}_{\text{POM}}$  (Fig. 1); this may be due to increased oil consumption at higher speeds. The average

and range of POM/BC observed here are consistent with both the low-sulfur and the all-vessels results from Lack et al. (2009) (POM/BC = 0.8 and 1.48, respectively), the plume intercept results from Lack et al. (2011) for the *Margrethe Maersk* (POM/BC = 1.3–2.6) and with two of the in-stack measurements: Jayaram et al. (2011) (POC/EC = 0.7–1.4) and Kasper et al. (2007) (POC/EC ~ 0.7–3), and where POC is particulate organic carbon and EC is elemental carbon. (It should be noted that EC is similar to, but not identical to BC, as both are defined based on the measurement method used. We assume here that BC is interchangeable with EC. See Petzold et al. (2013) for an extensive discussion. POC is related to POM, but excludes the mass of non-C atoms. We assume that POM/BC and POC/EC are sufficiently similar in magnitude such that they can be compared. This seems justified given that the POM/POC ratio for ship emissions was previously measured to be ~ 1.2, Murphy et al., 2009.) The POM/BC ratio observed here (and in the above-cited studies) is, however, substantially smaller than all other in-stack or test-rig studies, including results reported by Petzold and co-workers for a test-rig MSD operating on MGO (POM/EC = 3.6–8.7 and POM/BC = 6.9–77) (Petzold et al., 2011a) or heavy fuel oil (HFO) (POM/EC = 3.8–8.8 and POM/BC = 5.2–28) (Petzold et al., 2010), by Khan and co-workers for a slow-speed diesel (SSD) (POC/EC = 50–74) (Khan et al., 2012a) and MSD (POC/EC = 3–15) (Khan et al., 2012b) vessel operating on MGO, by Agrawal and co-workers for a few SSD vessels operating on HFO (POC/EC = 8–33) (Agrawal et al., 2008a, b, 2010) or an auxiliary engine operating on MGO (POC/EC = 3–10) (Agrawal et al., 2008b). Murphy et al. (2009) report EFs from a single SSD vessel operating on HFO using both in-stack and plume intercept methods and find values larger than those observed here, although with the in-stack POC/EC (= 25) nearly twice as large as the plume intercept POM/BC (= 13).

Plume intercept studies (this work; Lack et al., 2009, 2011; Murphy et al., 2009) measure the POM/BC ratio for emitted particles at atmospherically relevant dilutions while studies that utilize test rigs or that sample directly from the ship stack will sample at varying dilution factors that depend on the exact methodology employed. Thus, one possible reason for the difference between our results and some of the literature could be that the results depend on the methodology used, with ambient methods (i.e., plume sampling) typically giving lower POM/BC than direct sampling (e.g., in stack) measurement methods, likely due to the relatively rapid dilution experienced by a plume a few minutes downwind of emissions (Petzold et al., 2008) and consequent evaporation of semi-volatile POM species. Evaporation of POM may be greater in plume intercept studies compared with direct sampling, depending on the level of dilution used during sampling and the resultant POM concentrations. This suggestion is consistent with observations that have shown the dilution ratio used during sampling from diesel engines can have a

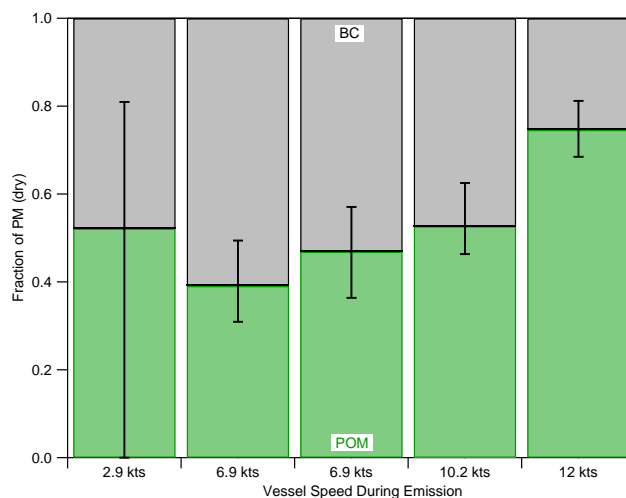


**Fig. 2.** The fraction of PM<sub>1</sub> that is BC (gray) or POM (green) as a function of vessel speed, determined from the weighted average POM and BC EFs.

profound influence on the amount of organic carbon measured and the POC/EC ratio (Lipsky and Robinson, 2006; Fujitani et al., 2012). Consider also that Murphy et al. (2009) found the POM/BC from plume intercepts to be about half that of the POC/EC measured via in-stack sampling for emissions from the same vessel. Given that EF<sub>BC</sub> is independent of dilution (since BC is non-volatile) while EF<sub>OM</sub> can be highly sensitive to dilution, our results, combined with literature results (e.g., Lack et al., 2009, 2011 and Murphy et al., 2009), indicate a potential for laboratory test-rig and stack-sampling methods to overestimate POM emission factors from ships and ship engines if sufficient dilution is not used during sampling. (It remains unclear why the Jayaram et al. (2011) stack-sampling and Kasper et al. (2007) test-rig studies give a similarly low POC/EC ratio.) Alternatively, it is possible that the difference between our low-sulfur fuel results and the literature studies that used heavy fuel oil could result from typically greater use of lubricating oil with HFO, which could translate to greater emissions of POM. However, this does not seem likely because the ensemble results from Lack et al. (2009), which include vessels with a variety of ages and types, suggest relatively small differences in the POM/BC ratio between ships operating on LSFs vs. HFO or between different engine types.

We note that this discussion is limited to primary POM emissions; the loss of POM due to evaporation leads to the production of gas-phase organic matter, which can photochemically react in the atmosphere on timescales longer than the plume transit times encountered here to produce secondary POM. Thus, it may be that POM is only temporarily lost, although the likelihood of re-condensation is dependent upon a variety of parameters, such as the concentration of gas-phase oxidants, temperature, relative humidity, dilution, etc. In addition to evaporation considerations, there may

be substantial differences (and large uncertainties) in the BC and EC measurements made using different techniques (Petzold et al., 2011b) that can also contribute to differences in reported POM/BC.

### 3.1.3 Particle number and size

Observed particle number concentration EFs ( $EF_{CN}$ ) for the *Miller Freeman* varied from  $1\text{--}3 \times 10^{16}$  particles  $\text{kg fuel}^{-1}$  (Table 1). The average  $EF_{CN}$  for all particles with diameters  $> 3$  nm were larger than for all particles with diameters  $> 12$  nm ( $2.3(\pm 0.5) \times 10^{16}$  vs.  $1.5(\pm 0.3) \times 10^{16}$  particles  $\text{kg fuel}^{-1}$ , respectively). The  $EF_{CN}$  exhibited no particular dependence on vessel speed, both for  $EF_{CN, > 3 \text{ nm}}$  and  $EF_{CN, > 12 \text{ nm}}$  (Fig. 1).

It was possible to determine mobility diameter size distributions associated with the emitted particles for some of the plumes from the SMPS measurements (Fig. 3). This was not possible for all plumes (specifically, the two 6.9 knot plumes) because, due to the narrowness of the plumes in time and the relative timing and long scan time of the SMPS, the plume-specific size distribution could not be resolved from the background (Fig. 3). The median number-weighted mobility diameter ( $d_{p,m}$ ) measured did exhibit some dependence on vessel speed, increasing from  $\sim 30$  nm at 2.9 knots, to 48 nm at 10 knots, to 69 nm at 12 knots. This observation is consistent with the observation that  $EF_{PM1}$  increased with vessel speed while  $EF_{CN}$  was speed independent (Fig. 1).

In addition to mobility size distributions, the SP2 was used to determine volume equivalent diameter number and mass-weighted size distributions for the rBC component of the particles from  $60 \text{ nm} < d_{p,VED} < 300 \text{ nm}$  (the detection limits of this SP2). For non-spherical, fractal-like particles  $d_{p,VED} < d_{p,m}$  (DeCarlo et al., 2004). The SP2 measures rBC size distributions with much higher time resolution than the SMPS making it possible to determine unique plume-specific size distributions for each intercept. The rBC number-weighted size distributions for the different plumes (Fig. 4) indicate that there is one mode that peaks at  $d_{p,VED} \sim 100$  nm and a second, much higher number concentration mode that maximizes at some diameter  $< 60$  nm. (It is important to note that the exact shape of the distributions below 100 nm is highly dependent upon the size-dependent counting efficiency correction applied; see Supplement for further details.) This is consistent with the rBC number concentrations in the plumes, as measured by the SP2, being only  $\sim 1\%$  of the total CN and with the observation that most of the particles existed with  $d_{p,m} < 100$  nm (Fig. 3). This also provides a rationale for the systematically smaller  $EF_{BC}$  values from the SP2 compared to the other measurement techniques.

Particle coagulation can strongly influence the measured  $EF_{CN}$ , with the extent to which this matters dependent upon both how rapidly and by how much the sample is diluted. Plume intercept observations have shown there can be a rapid

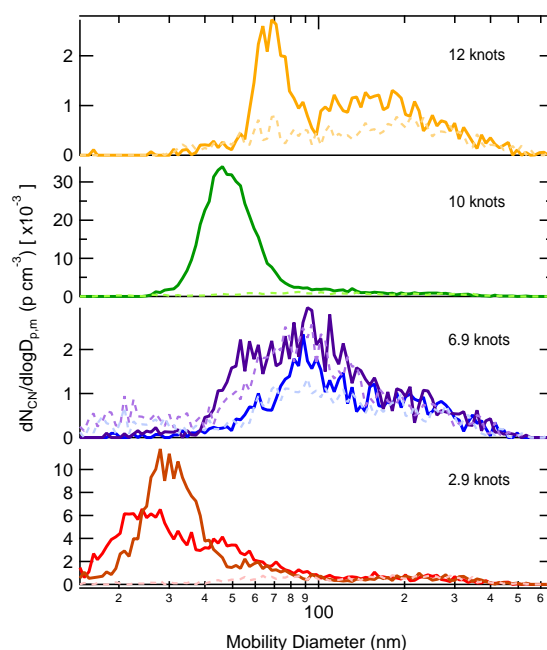


**Fig. 3.** Measured number-weighted particle mobility size distributions during plume intercepts at different vessel speeds. The solid lines indicate the distributions measured in the plumes while the dashed lines indicate distributions measured adjacent to the plumes and represent approximate background size distributions. The ability to distinguish plume distributions from background is not always apparent due to limited (random) overlap of the SMPS scanning cycle with the plume occurrence. However, for the 2.9, 10.2 and 12 knot intercepts a mode due to plume particles is clear. For the 2.9 knot intercept, the plume was sufficiently long that two full SMPS scans were completed, which are shown as independent size distributions.

shift in the ratio between  $EF_{CN, > 5 \text{ nm}}$  and  $EF_{CN, > 10 \text{ nm}}$  with distance downwind of the target vessel (Lack et al., 2009; Petzold et al., 2008). For the plumes intercepted here there is some correspondence between the measured  $EF_{CN}$  and plume age (Fig. 1d), consistent with these previous observations and providing additional evidence that coagulation plays an important role in determining the number concentration of particles in ship plumes. Given this, we suggest that the plume intercept method may be generally able to provide a more robust estimate of the absolute  $EF_{CN}$  most relevant to the atmosphere since it allows for determination of the EFs upon atmospherically relevant dilution factors and timescales. However, in-stack and test-rig studies may allow for a more straightforward measure of the influence of operating parameters (e.g., fuel type, speed/engine load) on the  $EF_{CN}$  because they can be conducted at constant dilution factors.

Comparing with literature plume intercept studies, both the  $EF_{CN}$  and the peak sizes of the particle size distributions measured here are similar to that observed by Lack et al. (2011) 2.5–7.5 min downwind for an ocean-going vessel

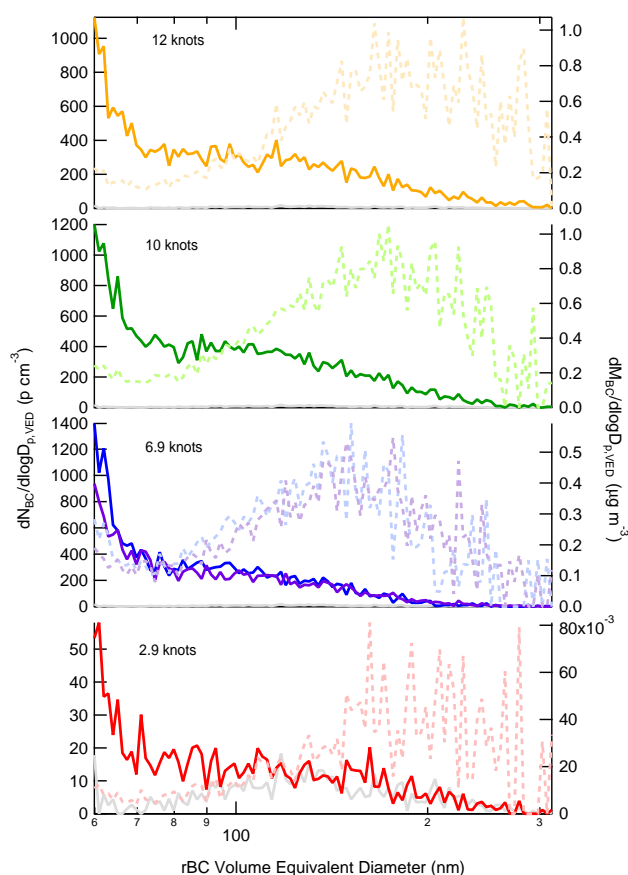


**Fig. 4.** Number-weighted (left axis and solid lines) and mass-weighted (right axis and dashed lines) size distributions for the rBC component of particles for each plume intercept, averaged over the entire plume. The number-weighted distributions for background (outside of plume) particles are shown as the grey traces in all panels. For all but the 2.9 knots plume the observed size distribution is well above the background. The speed of the R/V *Miller Freeman* corresponding to each plume is indicated on each panel.

operating a slow-speed diesel engine on HFO or MGO ( $EF_{CN, > 4\text{nm}} = 1.0\text{--}1.4 \times 10^{16}$  per kg fuel and  $d_{p,m} = 65\text{--}35$  nm). They also found that  $EF_{CN}$  was approximately constant while particle size increased with vessel speed for this vessel, although this occurred concurrent with a switch from operation on HFO to MGO, making it difficult to separate fuel quality (i.e., sulfur content) from vessel speed effects. The  $EF_{CN}$  here are also similar to the average observed by Petzold et al. (2008) from an SSD vessel operating on HFO at 85 % of max power when plume age > 16 min ( $EF_{CN, > 13\text{nm}} = 1.4 \times 10^{16}$  per kg fuel). The *Miller Freeman*  $EF_{CN}$  are somewhat larger than the ensemble average measurements of Lack et al. (2009) for MSD and SSD vessels operating on either LSF or HFO ( $EF_{CN, > 5\text{nm}} = 1.25 \times 10^{16}$  per kg fuel and  $EF_{CN, > 13\text{nm}} = 0.7 \times 10^{16}$  per kg fuel). Petzold et al. (2008) also report one measured size distribution for which  $d_{p,m} \sim 75$  nm, although they emphasized that the

size distribution may rapidly shift as a plume is increasingly diluted downwind.

Considering in-stack and test-rig studies, Khan et al. (2012a) observed a very slight increase in  $d_{p,m}$  with vessel speed at low speed ratios/loads for an SSD vessel operating on MGO. Kasper et al. (2007) observed a general, although not monotonic, increase in particle size with engine load for a SSD test rig operating on MDO, and that  $EF_{CN}$  was relatively constant for all  $F_{load} > 1\%$ . In contrast, Petzold et al. (2010), using HFO with an MSD test rig, observed a relatively continuous increase in  $EF_{CN}$  and decrease in particle size with engine load (although with some difference in  $EF_{CN}$  at  $F_{load} = 100\%$  before/after the engine had warmed up). However, in a separate study Petzold et al. (2011a) observed that  $EF_{CN}$  decreased with test-rig engine load for HFO operation, and that below  $F_{load} = 100\%$  the dependence of  $EF_{CN}$  on engine load was ambiguous for the same engine operating on various biofuels. Khan et al. (2012a) observed a strongly bimodal size distribution when a SSD vessel operated on HFO, but an approximately monomodal distribution when the same vessel operated on MGO. Additionally, they observed particle diameters were typically larger for HFO operation. Comparison of these various studies suggests that, in general, HFO operation tends to produce larger particles compared with LSF operation, consistent with the greater contribution of  $p\text{-SO}_4^{2-}$  to the total  $\text{PM}_{10}$  mass when HFO is utilized.

### 3.1.4 Cloud condensation nuclei

The above discussion illustrates that fuel type plays a strong role in determining the emitted particle size distribution. Developing clearer understanding of the impacts of vessel operating parameters, such as fuel type or speed, on  $EF_{CN}$  and particle size is critical to understanding sources of new particles to the atmosphere, and their potential to ultimately act as cloud condensation nuclei (CCN). Understanding the size dependence of emitted particles is important because the emitted size will determine the probability that a given emitted particle will survive to grow into the CCN active size range (Pierce and Adams, 2007).

Direct measurements of the  $EF_{CCN}$  were made for all particles with aerodynamic diameters less than  $1\ \mu\text{m}$  at super saturations (SS) ranging from 0.3–0.7 %. The CCN instrument operated in a mode wherein the SS was varied with time, and thus the measurements are not consistent across all of the plumes encountered. This makes it difficult to generalize the relationship between CCN number and vessel speed from these measurements. The best coverage was obtained for total sub-micrometer particles when  $SS = 0.6\%$  and  $0.7\%$ . The fraction of total CN that were CCN active at 0.6 % ranged from 0.004 to 0.007 and at 0.7 % ranged between 0.008–0.021 (see Table 1). These values are lower than those observed by Lack et al. (2009) at a lower SS, 0.44 %, for a variety of vessels operating on

higher sulfur fuel (CCN/CN = 0.42) or on fuel with < 0.5 % sulfur (CCN/CN = 0.07). They are also lower than observations at SS = 0.3 % for a single vessel as it operated on fuel with high sulfur content (~ 3 %; CCN/CN = 0.4), but are similar to observations for that same vessel operating on fuel with lower sulfur content (~ 0.2 %; CCN/CN = 0.007) (Lack et al., 2011); *Miller Freeman* was operating on fuel with sulfur content of ~ 0.1 % (see Sect. 3.2). It should be noted, however, that the higher SS used here should lead to overall higher CCN/CN, all other things being equal, which suggests that the CCN activity of the particles emitted by *Miller Freeman* was even lower than that observed by Lack et al. (2011) and is consistent with the  $\text{p-SO}_4^{2-}$  being a smaller fraction of the total PM in this study.

Our results indicate that directly emitted particles act inefficiently as CCN even at high super saturations (SS = 0.7 %). Additionally, there is less gas-phase sulfur emitted (Sect. 3.2) that could ultimately lead to downwind growth of the emitted particles. It is evident that the use of LSFs leads to substantially reduced emissions of both direct and potential CCN relative to higher sulfur fuels. As has been previously noted (Lauer et al., 2009; Lack et al., 2011; Righi et al., 2011), this reduction in CCN associated with shifts towards low-sulfur fuels has substantial implications for the likelihood of ship track formation and the current net cooling effect of PM emitted by ships – and thus for future regulation of the sulfur content of fuel used by ships. However, this climate impact must be balanced with the net benefits to air quality that derive from reductions in the emitted PM (Arneeth et al., 2009). It is also important to note that since the low-sulfur fuel in use by *Miller Freeman* had a sulfur content of only ~ 0.1 % these results are most applicable to vessels operating in sulfur emissions control areas in near-shore environments around California or the North and Baltic seas. Sulfur content for fuels in use by vessels on the high seas is currently limited by the IMO only to 3.5 %, and it has been suggested that this fuel sulfur restriction is leading to decreases in the maximum sulfur content of fuel used, but are having minimal influence on the average (Mestl et al., 2013).

### 3.1.5 Influence of vessel speed on emission

Opportunities to measure emissions from individual in-operation vessels, especially as a function of vessel speed, are rare and, as such, only a handful of case-studies are available (Agrawal et al., 2008aa, b, 2010; Jayaram et al., 2011; Khan et al., 2012a, b; Lack et al., 2011). This is particularly true for measurements of compositionally resolved PM emissions and for inter-comparisons of different techniques measuring the same pollutant.

Although decreased absolute emissions are expected as a result of the fuel economy increase as a vessel slows, there is not yet a clear understanding of how changes to vessel speed influences fuel-based emissions factors (EFs), i.e., the amount of pollutant emitted per kg fuel burned, although var-

ious studies using either laboratory test rigs or in-use stack sampling have provided insights (Agrawal et al., 2008a, b, 2010; Jayaram et al., 2011; Khan et al., 2012a, b; Petzold et al., 2008, 2010, 2011a). If EFs vary with vessel speed, then they may either enhance or decrease the effect of the increased fuel economy on the actual emissions ( $E_X$ ) because

$$E_X = \frac{EF_X}{F_{\text{econ}}} \times D, \quad (2)$$

where  $EF_X$  is the emission factor for pollutant  $X$  (in amount of  $X$  per kg fuel),  $D$  is the total distance travelled,  $F_{\text{econ}}$  is the fuel economy (km per kg fuel) and  $E_X$  is the absolute emissions; both  $EF_X$  and  $F_{\text{econ}}$  may be vessel speed dependent.

For the *Miller Freeman* the  $EF_{\text{POM}}$  and  $EF_{\text{BC}}$  both increase with vessel speed (Fig. 1). (All BC emission factors from the literature are for equivalent BC.) Since the emitted  $\text{PM}_{10}$  is dominated by POM and BC,  $EF_{\text{PM}_{10}}$  also increases with vessel speed. There have been a few previous measurements of vessel speed effects (or more commonly, engine load effects) on  $EF_{\text{BC}}$  for individual ships as measured in stack (Agrawal et al., 2008a, b, 2010; Jayaram et al., 2011; Khan et al., 2012a, b), for individual test rigs (Petzold et al., 2008, 2010, 2011a; Kasper et al., 2007; Sarvi and Zevenhoven, 2010; Sarvi et al., 2009) or for an ensemble of different ships using the plume intercept method (Lack et al., 2008b). (Note that some of these studies actually report  $EF_{\text{EC}}$ , where EC is elemental carbon. As above, we assume here that  $EF_{\text{BC}}$  is interchangeable with  $EF_{\text{EC}}$ .) These studies encompass slow-, medium- and high-speed diesel engines (SSD, MSD and HSD, respectively) of various types and a variety of different fuel types, including HFO, MGO, MDO and various biofuels. Most of the studies were done on vessels/engines substantially newer than the *Miller Freeman*. Propeller type was not reported for any of the in-stack studies, although for the in-stack studies that investigated larger ocean-going vessels it is likely that they operated fixed pitch propellers. (Propeller type does not apply to test-rig studies.) These differences present some challenges in making comparisons between different studies, including between the current study and the literature results. Nonetheless, it is instructional to consider the dependence observed here in the context of the literature results to gain insights into how differences in operation influence emissions, and absolute values can be compared independent of the actual speed dependence. We assume that for the literature studies the propeller law provides a reasonable method by which the ship speed (or potential ship speed, in the case of test-rig studies) can be estimated, or more specifically the ratio between the operating speed and the maximum speed (referred to here as the speed ratio). Therefore, the engine load values reported for the literature in-stack and test-rig studies have been converted to speed ratio values using the propeller law.

Adopting the approach of Lack and Corbett (2012) we present literature  $EF_{BC}$  (and  $EF_{EC}$ ) vs. speed ratio (either directly measured or estimated from the propeller law), and where either the absolute values of  $EF_{BC}$  are considered (Fig. 5b) or where the  $EF_{BC}$  values have been normalized to 95 % of their maximum speed (equivalent to 85 % load from the propeller law; Fig. 5a). It is important to compare EFs in the same units (here  $\text{g kg fuel}^{-1}$ ), and thus the literature results have been converted to  $\text{g kg fuel}^{-1}$  from  $\text{g kW}^{-1} \text{ h}^{-1}$ , as necessary (see Supplement for details of this conversion). It is evident that there is a great deal of scatter in the combined observations regarding the dependence of  $EF_{BC}$  on speed and it is difficult to develop generalized results, although it is clear that the *Miller Freeman* exhibits substantially different behavior than most other engines/vessels considered. This may be due to differences in propeller type between the *Miller Freeman* and other vessels. The absolute  $EF_{BC}$  values at higher speed ratios for the *Miller Freeman* are somewhat larger than most of the other individual ship studies, although they are within the multi-ship range of values observed by Lack et al. (2009) and are comparable to observations for other vessels encountered during CalNex (Buffaloe et al., 2013). At lower speed ratios the *Miller Freeman*  $EF_{BC}$  are well within the range of the individual ship studies.

Considering the literature results all together, there appears to be no clear distinction between studies that utilize SSD vs. MSD engines, or between those that use HFO vs. LSF. There does appear to be some small distinction between the majority of test-rig studies and the majority of stack-sampling studies; most test-rig studies (with the exception of Kasper et al., 2007) indicate a decrease in  $EF_{BC}$  with increasing speed ratio while most stack-sampling studies (with the exception of Jayaram et al., 2011) suggest flat or slightly decreasing  $EF_{BC}$  with speed ratio.

The present work is the only plume-intercept study that involved a single ship and is most consistent with the Kasper et al. (2007) lab study and the Jayaram et al. (2011) stack-sampling study (with the exception of the lowest speed ratio, which for Jayaram et al. was “idle” while in ours it was slow travel). The reason for the apparent similarity of the current work with these particular studies is not clear because they had used the same, or very similar, sampling methodologies as the other stack-sampling and test-rig studies. This may simply be an indication of the study-to-study variability. The ensemble study of Lack et al. (2008b), in which EFs were determined from plume intercepts from multiple ships (excluding tugs), with each ship typically sampled at one single speed, does not suggest a clear dependence of  $EF_{BC}$  on speed; this may simply reflect that the ship-to-ship variability is larger than any vessel speed/engine load effect and demonstrates the need for further studies that focus on the behavior of individual vessels.

Literature results for  $EF_{POM}$  (or  $EF_{POC}$ ) as a function of speed ratio are shown normalized to 95 % (Fig. 6a) or as absolute values (Fig. 6b). As with  $EF_{BC}$ , there is a great deal

of scatter in the  $EF_{POM}$ /speed relationships, although with most literature studies suggesting an increase or being relatively flat in the  $EF_{POM}$  at low speed ratios, different than the current study. This may reflect differences in engine/vessel operating conditions. Our results are again most consistent with the test-rig MGO results from Kasper et al. (2007), who observed an increase in  $EF_{POM}$  with estimated speed. Also as with  $EF_{BC}$ , there is a great deal of scatter between the various studies in terms of the absolute  $EF_{POM}$  values. As discussed in Sect. 3.1.2,  $EF_{POM}$  measurements may be influenced by the extent of dilution during sampling, although it is not clear how this might influence observations of the  $EF_{POM}$ /speed dependence.

Despite the large number of points in Figs. 5 and 6, only a handful of different engines have actually been tested, which leaves an open question of the general dependence of  $EF_{BC}$  and  $EF_{POM}$  on vessel speed (and engine load), or whether generalizations can even be determined. We suggest more plume intercept studies targeting individual vessels would be beneficial, although coordinating such studies for measurement of emissions from individual vessels (as in this study) is extremely difficult, requiring multiple platforms. Additionally, use of a variety of instrumentation to measure BC (or EC) is suggested.

### 3.2 Gas-phase emissions

EFs for gas-phase species are shown in Fig. 7 and given in Table 1.  $EF_{CO}$  decreased with increasing vessel speed by approximately a factor of 3 over the range considered here. In contrast,  $EF_{NO_x}$  increased with increasing vessel speed by approximately 20 %. These results are expected since higher speed operation would likely have resulted in higher peak combustion temperatures and, therefore, greater NO formation and lower CO production. Since diesel engines typically operate under fuel lean conditions, if the fuel-to-air ratio did increase with vessel speed, as we postulated earlier, this would likely accentuate the  $NO_x$  increase but have minimal influence on CO. The  $EF_{HCHO}$  are inversely correlated with  $F_{load}$ . For all but the lowest speed plume, the relationship between  $EF_{CO}$  and  $EF_{HCHO}$  is consistent with previous observations from Williams et al. (2009). Our observations of  $EF_{NO_x}$  and  $EF_{CO}$  exhibit the opposite dependence of that observed by Khan et al. (2012a) for operation of a SSD engine on MGO, although agree with their observations when the ship operated on HFO. For comparison, Agrawal et al. (2010) found little dependence of CO or  $NO_x$  EFs on engine load for a SSD container ship operating on HFO. The reason for these differences is unclear, but could be related to engine or propeller type. Our results for CO suggest that, for smaller vessels such as the *Miller Freeman*, the decrease in absolute emissions from increased fuel economy at reduced speeds may be offset to some extent by an increase in  $EF_{CO}$ , whereas the decrease in  $EF_{NO_x}$  may enhance emissions reductions.

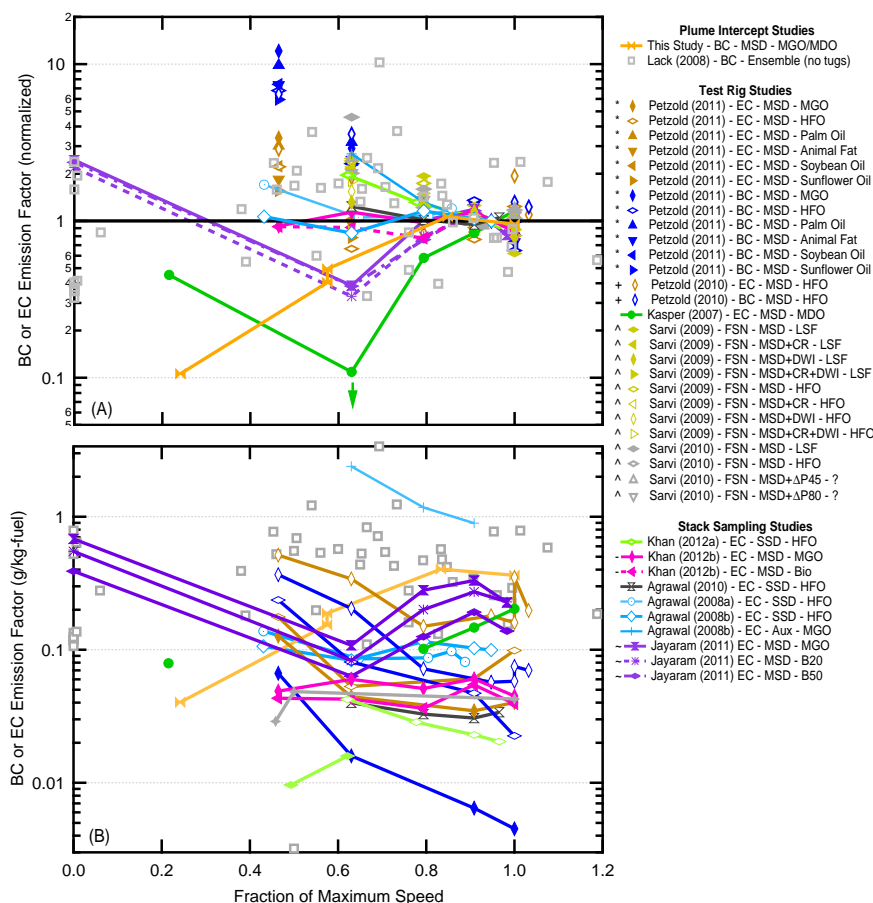


**Fig. 5.** Emissions factors (in g per kg fuel) for black carbon (BC), elemental carbon (EC) or the “filter smoke number” (FSN) as a function of the vessel speed ratio for multiple studies (A) normalized to a speed ratio of 95 % (which corresponds to 85 % load using the propeller law) load and (B) as absolute values. All BC emission factors correspond to equivalent BC, with the exception of the current study, which is the uncertainty weighted-average from the four measurement methods. The speed ratio is the ratio between the operating speed and the maximum ship speed, and for the test-rig and stack-sampling studies was estimated from the reported engine load using the propeller law. The legend groups the studies by measurement methodology: plume intercept, test-rig and stack sampling. The symbols in the legend indicate which studies were performed on the same engine or ship. The legend names indicate the study, measured parameter (BC, EC or FSN), engine type (MSD or SSD) and fuel type (HFO or low-sulfur, including biofuels, MDO and MGO). For the Sarvi studies, the additional information given after the engine type indicates a variation in the engine operation over the base case and includes use of a common rail injection system (CR), direct water injection (DWI), or variation in the fuel nozzle open pressure ( $\Delta P$ ). The downward green arrow indicates that the actual EF reported for this point was actually zero.

The values of  $EF_{SO_2}$  were independent of vessel speed. We would not expect  $EF_{SO_2}$  to depend strongly on engine load since it is primarily dependent on the sulfur content of the fuel. This is similar behavior as observed by Khan et al. (2012a). The low value of  $EF_{SO_2}$  confirms that *Miller Freeman* was indeed burning low-sulfur fuel, which we estimate to be  $0.097 \pm 0.011$  % sulfur by weight based upon the average  $EF_{SO_2}$ , a negligible EF for  $p\text{-SO}_4^{2-}$  and the assumption that  $SO_3$  emissions are very small.

#### 4 Implications

Our results provide a useful case study of the dependence of PM and trace gas emissions factors on vessel speed as measured from a real-world MSD vessel, representative of many harbor craft vessels operating on low-sulfur fuel. The observed increase in PM mass EFs with vessel speed suggests that slower speed operation of these vessel types may lead to substantially lower emissions, especially since slower speed operation also corresponds to (typically) better fuel economy. One aspect not considered here is that harbor craft vessels operating near-shore or in inland waterways may be subject to frequent speed changes, and we do not have measurements

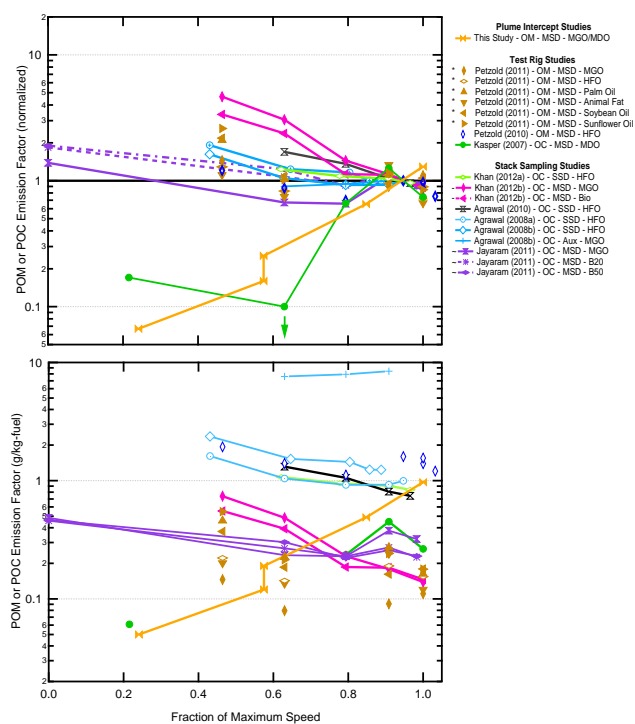


**Fig. 6.** Emissions factors (in g per kg fuel) for primary organic matter (POM) or primary organic carbon (POC) as a function of the vessel speed ratio for multiple studies (A) normalized to 85 % load and (B) as absolute values. The speed ratio is the ratio between the operating speed and the maximum ship speed, and for the test-rig and stack-sampling studies was estimated from the reported engine load using the propeller law. The symbols in the legend indicate which studies were performed on the same engine or ship. The legend names indicate the study, reported parameter (POM or POC), engine type (MSD or SSD) and fuel type (HFO or low-sulfur, including biofuels, MDO and MGO). The downward green arrow indicates that the actual EF reported for this point was actually zero.

as to how the EFs respond to rapid acceleration; we suggest such measurements would be useful in future studies.

More broadly, comparison with literature results demonstrates that challenges exist in developing a generalized EF/speed (or engine load) relationship, in particular for PM emissions, because results from individual studies may depend on the measurement methodology used: plume intercept (this study and others (Lack et al., 2008b, 2009, 2011; Petzold et al., 2008)) vs. in-use stack sampling (Agrawal et al., 2008a, 2010; Jayaram et al., 2011; Khan et al., 2012a, b; Murphy et al., 2009) vs. test-rig sampling (Petzold et al., 2010, 2011a; Sarvi et al., 2009; Sarvi and Zevenhoven, 2010; Kasper et al., 2007). This is true even if the current study is excluded. Also, it is clear that there is a great deal of variability in the absolute emissions between different vessels, perhaps not surprising given the variety of different engine types and ages considered in the various studies (Table S1). Methodological limitations, along with the limited number

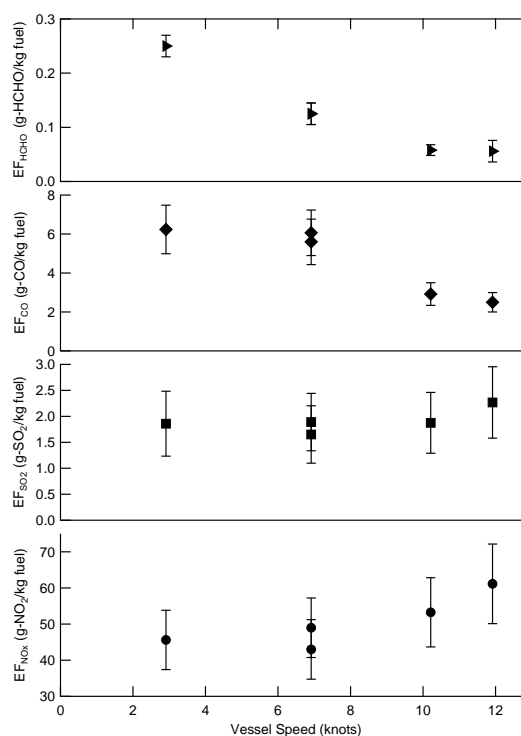


**Fig. 7.** Measured emissions factors, in g-X per kg fuel for (top to bottom) HCHO, CO, SO<sub>2</sub> and NO<sub>x</sub> (as NO<sub>2</sub>) as a function of vessel speed.

of different vessels or engines for which measurements have been made, makes it difficult to establish whether engine type or fuel type affects the EF/speed relationship. Although logistically more challenging, we suggest that plume intercept studies, which allow for measurement of EFs under actual atmospheric dilution conditions, may provide for EFs that are most relevant to the actual atmosphere, and thus to emission inventory development. We additionally suggest that, whenever possible, multiple measurement techniques be employed, especially for BC (or EC). Our measurement of BC EFs at atmospheric relevant dilution levels using multiple methodologies (e.g., photo-acoustics, filter-based absorption, laser induced incandescence and aerosol mass spectrometry) suggest that the SP2 underestimates BC emissions relative to other methods, likely due to methodological limitations. We suggest that, barring additional improvements in field-deployable laser-induced incandescence methods (e.g., Chan et al., 2011), that light absorption techniques may provide the most robust and accurate determination of EF<sub>BC</sub>. Further consideration of the influence of vessel speed and engine load on other engine and ship types remains necessary.

**Supplementary material related to this article is available online at <http://www.atmos-chem-phys.net/14/1337/2014/acp-14-1337-2014-supplement.pdf>.**

**Acknowledgements.** The authors thank the crews of the R/V *Atlantis* and the *Miller Freeman*, especially the Field Operations Officer on the *Miller Freeman* P. Murphy, without all of whom this study would not have been possible. This work was supported in part by the US Environmental Protection Agency under a STAR research assistance agreement (RD834558), the NOAA Climate Program (including NA09OAR4310124 and NA09AR4310125), the California Air Resources Board, the Canadian Federal Government (PERD Project C12.007) and NSERC. It has not been formally reviewed by the any of the funding agencies. The views expressed in this document are solely those of the authors, and the funding agencies do not endorse any products or commercial services mentioned in this publication.

Edited by: D. Topping

## References

- Agrawal, H., Malloy, Q. G. J., Welch, W. A., Miller, J. W., and Cocker III, D. R.: In-use gaseous and particulate matter emissions from a modern ocean going container vessel, *Atmos. Environ.*, 42, 5504–5510, doi:10.1016/j.atmosenv.2008.02.053, 2008a.
- Agrawal, H., Welch, W. A., Miller, J. W., and Cocker III, D. R.: Emission measurements from a crude oil tanker at sea, *Environ. Sci. Technol.*, 42, 7098–7103, doi:10.1021/es703102y, 2008b.
- Agrawal, H., Welch, W. A., Henningsen, S., Miller, J. W., and Cocker III, D. R.: Emissions from main propulsion engine on container ship at sea, *J. Geophys. Res.-Atmos.*, 115, D23205, doi:10.1029/2009jd013346, 2010.
- Arnth, A., Unger, N., Kulmala, M., and Andreae, M. O.: Clean the Air, Heat the Planet?, *Science*, 326, 672–673, doi:10.1126/science.1181568, 2009.
- Bond, T. C. and Bergstrom, R. W.: Light absorption by carbonaceous particles: An investigative review, *Aerosol Sci. Tech.*, 40, 27–67, doi:10.1080/02786820500421521, 2006.
- Buffaloe, G. M., Lack, D. A., Williams, E. J., Coffman, D., Hayden, K. L., Lerner, B. M., Li, S.-M., Nuaaman, I., Massoli, P., Onasch, T. B., Quinn, P. K., and Cappa, C. D.: Black carbon emissions from in-use ships: a California regional assessment, *Atmos. Chem. Phys. Discuss.*, 13, 24675–24712, doi:10.5194/acpd-13-24675-2013, 2013.
- Buhaus, O., Corbett, J. J., Endresen, O., Eyring, V., Faber, J., Hanayama, S., Lee, D. S., Lee, D., Lindstad, H., Mjelde, A., Palsson, C., Wanquing, W., Winebrake, J. J., and Yoshida, K.: Second IMO Greenhouse Gas Study, International Maritime Organization, London, 2009.
- California Air Resources Board, Final Regulation Order, Fuel Sulphur and Other Operational Requirements for Ocean-Going Vessels Within California Waters and 24 Nautical Miles of the California Baseline, available at: <http://www.arb.ca.gov/regact/2011/ogv11/ogvfro13.pdf> (last access: 17 June 2013), 2011.
- Cappa, C. D., Lack, D. A., Burkholder, J. B., and Ravishankara, A. R.: Bias in filter-based aerosol light absorption measurements due to organic aerosol loading: Evidence from laboratory measurements, *Aerosol Sci. Tech.*, 42, 1022–1032, doi:10.1080/02786820802389285, 2008.
- Chan, T. W., Brook, J. R., Smallwood, G. J., and Lu, G.: Time-resolved measurements of black carbon light absorption enhancement in urban and near-urban locations of southern Ontario, Canada, *Atmos. Chem. Phys.*, 11, 10407–10432, doi:10.5194/acp-11-10407-2011, 2011.
- Corbett, J. J. and Fischbeck, P. S.: Emissions from Waterborne Commerce Vessels in United States Continental and Inland Waterways, *Environ. Sci. Technol.*, 34, 3254–3260, doi:10.1021/es9911768, 2000.
- Corbett, J. J., Winebrake, J. J., Green, E. H., Kasibhatla, P., Eyring, V., and Lauer, A.: Mortality from Ship Emissions: A Global Assessment, *Environ. Sci. Technol.*, 41, 8512–8518, doi:10.1021/es071686z, 2007.
- Corbett, J. J., Wang, H., and Winebrake, J. J.: The effectiveness and costs of speed reductions on emissions from international shipping, *Transport. Res. D-Tr. E.*, 14, 593–598, doi:10.1016/j.trd.2009.08.005, 2009.
- DeCarlo, P. F., Slowik, J. G., Worsnop, D., Davidovits, P., and Jimenez, J. L.: Particle morphology and density characterization by combined mobility and aerodynamic diameter measurements. Part I: Theory, *Aerosol Sci. Tech.*, 38, 1185–1205, doi:10.1080/027868290903907, 2004.
- Equasis, The World Merchant Fleet in 2011, Statistics from Equasis, available at: [www.emsa.europa.eu/news-a-press-centre/download/1933/1554/23.html](http://www.emsa.europa.eu/news-a-press-centre/download/1933/1554/23.html) (last access: 21 May 2013), 2012.
- Fuglestedt, J., Berntsen, T., Eyring, V., Isaksen, I., Lee, D. S., and Sausen, R.: Shipping Emissions: From Cooling to Warming of Climate – and Reducing Impacts on Health, *Environ. Sci. Technol.*, 43, 9057–9062, doi:10.1021/es901944r, 2009.
- Fujitani, Y., Saitoh, K., Fushimi, A., Takahashi, K., Hasegawa, S., Tanabe, K., Kobayashi, S., Furuyama, A., Hirano, S., and Takami, A.: Effect of isothermal dilution on emission factors of organic carbon and n-alkanes in the particle and gas phases of diesel exhaust, *Atmos. Environ.*, 59, 389–397, doi:10.1016/j.atmosenv.2012.06.010, 2012.
- Hand, J. L. and Malm, W. C.: Review of aerosol mass scattering efficiencies from ground-based measurements since 1990, *J. Geophys. Res.-Atmos.*, 112, D16203, doi:10.1029/2007JD008484, 2007.
- Huffman, J. A., Jayne, J., Drewnick, F., Aiken, A. C., Onasch, T., and Worsnop, D.: Design, modeling, optimization and experimental tests of a particle beam width probe for the Aerodyne aerosol mass spectrometer, *Aerosol Sci. Tech.*, 39, 1143–1163, doi:10.1080/02786820500423782, 2005.
- International Maritime Organization, MARPOL Annex VI: Sulphur oxides (SO<sub>x</sub>) – Regulation 14, available at: <http://www.imo.org/OurWork/Environment/PollutionPrevention/AirPollution/Pages/Sulphur-oxides-%28SOx%29-%E2%80%9393-Regulation-14.aspx> (last access: 16 December 2013), 2013.
- Jayaram, V., Agrawal, H., Welch, W. A., Miller, J. W., and Cocker, D. R.: Real-Time Gaseous, PM and Ultrafine Particle Emissions from a Modern Marine Engine Operating on Biodiesel, *Environ. Sci. Technol.*, 45, 2286–2292, doi:10.1021/es1026954, 2011.
- Kasper, A., Aufdenblatten, S., Forss, A., Mohr, M., and Burtscher, H.: Particulate Emissions from a Low-Speed Marine Diesel Engine, *Aerosol Sci. Tech.*, 41, 24–32, doi:10.1080/02786820601055392, 2007.
- Khan, M. Y., Giordano, M., Gutierrez, J., Welch, W. A., Asa-Awuku, A., Miller, J. W., and Cocker, D. R.: Benefits of two mitigation strategies for container vessels: cleaner en-

- gines and cleaner fuels, *Environ. Sci. Technol.*, 46, 5049–5056, doi:10.1021/es2043646, 2012a.
- Khan, M. Y., Russell, R. L., Welch, W. A., Cocker, D. R., and Ghosh, S.: Impact of Algae Biofuel on In-Use Gaseous and Particulate Emissions from a Marine Vessel, *Energ. Fuel.*, 26, 6137–6143, doi:10.1021/ef300935z, 2012b.
- Laborde, M., Mertes, P., Zieger, P., Dommen, J., Baltensperger, U., and Gysel, M.: Sensitivity of the Single Particle Soot Photometer to different black carbon types, *Atmos. Meas. Tech.*, 5, 1031–1043, doi:10.5194/amt-5-1031-2012, 2012.
- Lack, D. A. and Corbett, J. J.: Black carbon from ships: a review of the effects of ship speed, fuel quality and exhaust gas scrubbing, *Atmos. Chem. Phys.*, 12, 3985–4000, doi:10.5194/acp-12-3985-2012, 2012.
- Lack, D. A., Cappa, C. D., Covert, D. S., Baynard, T., Massoli, P., Sierau, B., Bates, T. S., Quinn, P. K., Lovejoy, E. R., and Ravishankara, A. R.: Bias in filter-based aerosol light absorption measurements due to organic aerosol loading: Evidence from ambient measurements, *Aerosol Sci. Tech.*, 42, 1033–1041, doi:10.1080/02786820802389277, 2008a.
- Lack, D. A., Lerner, B., Granier, C., Baynard, T., Lovejoy, E., Massoli, P., Ravishankara, A. R., and Williams, E.: Light absorbing carbon emissions from commercial shipping, *Geophys. Res. Lett.*, 35, L13815, doi:10.1029/2008gl033906, 2008b.
- Lack, D. A., Corbett, J. J., Onasch, T., Lerner, B., Massoli, P., Quinn, P. K., Bates, T. S., Covert, D. S., Coffman, D., Sierau, B., Herndon, S., Allan, J., Baynard, T., Lovejoy, E., Ravishankara, A. R., and Williams, E.: Particulate emissions from commercial shipping: Chemical, physical, and optical properties, *J. Geophys. Res.-Atmos.*, 114, D00F04, doi:10.1029/2008jd011300, 2009.
- Lack, D. A., Cappa, C. D., Langridge, J., Bahreni, R., Buffaloe, G., Brock, C. A., Cerully, K., Hayden, K., Holloway, J. S., Lerner, B., Li, S. M., McLaren, R., Middlebrook, A., Moore, R., Nenes, A., Nuaanman, I., Peischl, J., Perring, A., Quinn, P. K., Ryerson, T. B., Schwarz, J. P., Spackman, J. R., and Williams, E. J.: Impact of Fuel Quality Regulation and Speed Reductions on Shipping Emissions: Implications for Climate and Air Quality, *Environ. Sci. Technol.*, 45, 9052–9060, doi:10.1021/es2013424, 2011.
- Lack, D. A., Richardson, M. S., Law, D., Langridge, J. M., Cappa, C. D., and Murphy, D. M.: Aircraft instrumentation for comprehensive characterization of aerosol optical properties, Part 2: Black and brown carbon absorption and absorption enhancement measured with photo acoustic spectroscopy, *Aerosol Sci. Tech.*, 46, 555–568, doi:10.1080/02786820600803917, 2012.
- Langridge, J. M., Richardson, M. S., Lack, D., Law, D., and Murphy, D. M.: Aircraft Instrument for Comprehensive Characterization of Aerosol Optical Properties, Part I: Wavelength-Dependent Optical Extinction and Its Relative Humidity Dependence Measured Using Cavity Ringdown Spectroscopy, *Aerosol Sci. Technol.*, 45, 1305–1318, doi:10.1080/02786826.2011.592745, 2011.
- Lauer, A., Eyring, V., Corbett, J. J., Wang, C., and Winebrake, J. J.: Assessment of Near-Future Policy Instruments for Ocean-going Shipping: Impact on Atmospheric Aerosol Burdens and the Earth's Radiation Budget, *Environ. Sci. Technol.*, 43, 5592–5598, doi:10.1021/es900922h, 2009.
- Liggio, J., Gordon, M., Smallwood, G., Li, S.-M., Stroud, C., Staebler, R., Lu, G., Lee, P., Taylor, B., and Brook, J. R.: Are Emissions of Black Carbon from Gasoline Vehicles Underestimated? Insights from Near and On-Road Measurements, *Environ. Sci. Technol.*, 46, 4819–4828, doi:10.1021/es2033845, 2012.
- Lipsky, E. M. and Robinson, A. L.: Effects of dilution on fine particle mass and partitioning of semivolatile organics in diesel exhaust and wood smoke, *Environ. Sci. Technol.*, 40, 155–162, doi:10.1021/es050319p, 2006.
- Lloyd's Register Engineering Services: Marine Exhaust Emissions Research Programme, London, 1995.
- Matthew, B. M., Middlebrook, A. M., and Onasch, T. B.: Collection efficiencies in an Aerodyne Aerosol Mass Spectrometer as a function of particle phase for laboratory generated aerosols, *Aerosol Sci. Tech.*, 42, 884–898, doi:10.1080/02786820802356797, 2008.
- McLaren, R., Wojtal, P., Halla, J. D., Mihele, C., and Brook, J. R.: A survey of NO<sub>2</sub>:SO<sub>2</sub> emission ratios measured in marine vessel plumes in the Strait of Georgia, *Atmos. Environ.*, 46, 655–658, doi:10.1016/j.atmosenv.2011.10.044, 2012.
- Mestl, T., Løvøll, G., Stensrud, E., and Le Breton, A.: The Doubtful Environmental Benefit of Reduced Maximum Sulfur Limit in International Shipping Fuel, *Environ. Sci. Technol.*, 47, 6098–6101, doi:10.1021/es4009954, 2013.
- Murphy, S. M., Agrawal, H., Sorooshian, A., Padro, L. T., Gates, H., Hersey, S., Welch, W. A., Jung, H., Miller, J. W., Cocker, D. R., Nenes, A., Jonsson, H. H., Flagan, R. C., and Seinfeld, J. H.: Comprehensive Simultaneous Shipboard and Airborne Characterization of Exhaust from a Modern Container Ship at Sea, *Environ. Sci. Technol.*, 43, 4626–4640, doi:10.1021/es802413j, 2009.
- NOAA, Miller Freeman, available at: [http://www.moc.noaa.gov/mf/apr\\_2004\\_mf\\_specs.pdf](http://www.moc.noaa.gov/mf/apr_2004_mf_specs.pdf) (last access: 10 January 2011), 2010.
- Onasch, T. B., Trimborn, A. M., Fortner, E. C., Jayne, J. T., Kok, G. L., Williams, L. R., Davidovits, P., and Worsnop, D. R.: Soot Particle Aerosol Mass Spectrometer: Development, Validation and Initial Application, *Aerosol Sci. Tech.*, 46, 804–817, doi:10.1080/02786826.2012.663948, 2012.
- Petzold, A., Hasselbach, J., Lauer, P., Baumann, R., Franke, K., Gurk, C., Schlager, H., and Weingartner, E.: Experimental studies on particle emissions from cruising ship, their characteristic properties, transformation and atmospheric lifetime in the marine boundary layer, *Atmos. Chem. Phys.*, 8, 2387–2403, doi:10.5194/acp-8-2387-2008, 2008.
- Petzold, A., Weingartner, E., Hasselbach, I., Lauer, P., Kurok, C., and Fleischer, F.: Physical Properties, Chemical Composition, and Cloud Forming Potential of Particulate Emissions from a Marine Diesel Engine at Various Load Conditions, *Environ. Sci. Technol.*, 44, 3800–3805, doi:10.1021/es903681z, 20110.
- Petzold, A., Lauer, P., Fritsche, U., Hasselbach, J., Lichtenstern, M., Schlager, H., and Fleischer, F.: Operation of Marine Diesel Engines on Biogenic Fuels: Modification of Emissions and Resulting Climate Effects, *Environ. Sci. Technol.*, 45, 10394–10400, doi:10.1021/es2021439, 2011a.
- Petzold, A., Marsh, R., Johnson, M., Miller, M., Sevcenco, Y., Delhaye, D., Ibrahim, A., Williams, P., Bauer, H., Crayford, A., Bachalo, W. D., and Raper, D.: Evaluation of Methods for Measuring Particulate Matter Emissions from Gas Turbines, *Environ. Sci. Technol.*, 45, 3562–3568, doi:10.1021/es103969v, 2011b.
- Petzold, A., Ogren, J. A., Fiebig, M., Laj, P., Li, S.-M., Baltensperger, U., Holzer-Popp, T., Kinne, S., Pappalardo, G., Sugimoto, N., Wehrli, C., Wiedensohler, A., and Zhang, X.-Y.: Rec-

- ommendations for reporting “black carbon” measurements, *Atmos. Chem. Phys.*, 13, 8365–8379, doi:10.5194/acp-13-8365-2013, 2013.
- Pierce, J. R. and Adams, P. J.: Efficiency of cloud condensation nuclei formation from ultrafine particles, *Atmos. Chem. Phys.*, 7, 1367–1379, doi:10.5194/acp-7-1367-2007, 2007.
- Righi, M., Klinger, C., Eyring, V., Hendricks, J., Lauer, A., and Petzold, A.: Climate Impact of Biofuels in Shipping: Global Model Studies of the Aerosol Indirect Effect, *Environ. Sci. Technol.*, 45, 3519–3525, doi:10.1021/es1036157, 2011.
- Roberts, G. C. and Nenes, A.: A continuous-flow streamwise thermal-gradient CCN chamber for atmospheric measurements, *Aerosol Sci. Tech.*, 39, 206–221, doi:10.1080/027868290913988, 2005.
- Ryerson, T. B., Andrews, A. E., Angevine, W. M., Bates, T. S., Brock, C. A., Cairns, B., Cohen, R. C., Cooper, O. R., De Gouw, J. A., Fehsenfeld, F. C., Ferrare, R. A., Fischer, M. L., Flagan, R. C., Goldstein, A. H., Hair, J. W., Hardesty, R. M., Hostetler, C. A., Jimenez, J. L., Langford, A. O., McCauly, E., McKeen, S. A., Molina, L. T., Nenes, A., Oltmans, S. J., Parrish, D. D., Pederson, J. R., Pierce, R. B., Prather, K., Quinn, P. K., Seinfeld, J. H., Senff, C. J., Sorooshian, A., Stutz, J., Surratt, J. D., Trainer, M., Volkamer, R. M., Williams, E. J., and Wofsy, S. C.: The 2010 California Research at the Nexus of Air Quality and Climate Change (CalNex) Field Study, *J. Geophys. Res.-Atmos.*, 118, 5830–5866, doi:10.1002/jgrd.50331, 2013.
- Sarvi, A. and Zevenhoven, R.: Large-scale diesel engine emission control parameters, *Energy*, 35, 1139–1145, doi:10.1016/j.energy.2009.06.007, 2010.
- Sarvi, A., Kilpinen, P., and Zevenhoven, R.: Emissions from large-scale medium-speed diesel engines: 3. Influence of direct water injection and common rail, *Fuel Process. Technol.*, 90, 222–231, doi:10.1016/j.fuproc.2008.09.003, 2009.
- Schwarz, J. P., Gao, R. S., Fahey, D. W., Thomson, D. S., Watts, L. A., Wilson, J. C., Reeves, J. M., Darbeheshti, M., Baumgardner, D. G., Kok, G. L., Chung, S. H., Schulz, M., Hendricks, J., Lauer, A., Karcher, B., Slowik, J. G., Rosenlof, K. H., Thompson, T. L., Langford, A. O., Loewenstein, M., and Aikin, K. C.: Single-particle measurements of midlatitude black carbon and light-scattering aerosols from the boundary layer to the lower stratosphere, *J. Geophys. Res.-Atmos.*, 111, D16207, doi:10.1029/2006jd007076, 2006.
- Schwarz, J. P., Spackman, J. R., Gao, R. S., Perring, A. E., Cross, E., Onasch, T. B., Ahern, A., Wrobel, W., Davidovits, P., Olfert, J., Dubey, M. K., Mazzoleni, C., and Fahey, D. W.: The Detection Efficiency of the Single Particle Soot Photometer, *Aerosol Sci. Tech.*, 44, 612–628, doi:10.1080/02786826.2010.481298, 2010.
- United Nations Conference on Trade and Development: Structure, Ownership and Registration of the World Fleet, in: *Review of Maritime Transport*, 2011.
- US EPA, Designation of North American Emission Control Area to Reduce Emissions from Ships, EPA-420-F-10-015, available at: <http://www.epa.gov/otaq/regs/nonroad/marine/ci/420f10015.pdf> (last access: 23 March 2013), 2010.
- Virkkula, A., Ahlquist, N. C., Covert, D. S., Arnott, W. P., Sheridan, P. J., Quinn, P. K., and Coffman, D. J.: Modification, calibration and a field test of an instrument for measuring light absorption by particles, *Aerosol Sci. Tech.*, 39, 68–83, doi:10.1080/027868290901963, 2005.
- Wang, H. and Minjares, R.: Global emissions of marine black carbon: critical review and revised assessment, 92nd Transportation Research Board Annual Meeting, <http://docs.trb.org/prp/13-1503.pdf> (last access: 30 January 2014), 2013.
- Williams, E. J., Lerner, B. M., Murphy, P. C., Herndon, S. C., and Zahniser, M. S.: Emissions of NO<sub>x</sub>, SO<sub>2</sub>, CO, and HCHO from commercial marine shipping during Texas Air Quality Study (TexAQS) 2006, *J. Geophys. Res.-Atmos.*, 114, D21306, doi:10.1029/2009jd012094, 2009.